Aalborg University

School of Engineering and Science

Department of Chemistry and Bioscience

Molecular Imprinted Particles

Three different methodologies for the specific recognition of saccharides in aqueous solutions

Master's Thesis

Rasmus Frandsen

[This page is intentionally left blank]

The Faculty of Engineering and Science
Chemical Engineering
Frederik Bajers Vej 7H
9000 Aalborg, DK
Phone: 99 40 36 05
www.bio.aau.dk

Title: Molecular Imprinted Particles
Three different methodologies for the specific recognition of saccharides in aqueous solutions

Semester: 3-4. semester

Project period: Spring

Participants:
Rasmus Frandsen _____

Supervisor: Donghong Yu
Department of Chemistry and Bioscience
Section for Chemistry

Appendices: Raw data is provided as electronic supplementary

[This page is intentionally left blank]

Molecular Imprinted Particles

Three different methodologies for the specific recognition of saccharides in aqueous solutions

Rasmus Frandsen

Master Thesis in Chemical Engineering, Department of Chemistry and Bioscience, Aalborg University

Abstract

The field of molecular imprinting has seen increasing interest in the last years, with the goal of producing highly selective receptors reminiscent of those found in biological systems, albeit with the tolerance and versatility of plastics. Due to its simplicity, molecular imprinting is most often done by bulk polymerization. Expanding the applicability of the technique requires a wider range of polymerization methods. Specific recognition of sacchrides is of special interest for blood glucose monitoring for diabetic patients and early cancer detection. In this study three different methodologies for the synthesis of molecularly imprinting particles were explored with the goal of selective rebinding of saccharides under aqueous conditions using Alizarin Red S as a model analyte. Particles were successfully synthesised by: 1) Nano particle stabilized emulsion polymerization, 2) Conventional emulsion polymerization incorporating a template phase transfer system, and 3) Core-shell polymerization. While particles afforded by the conventional emulsion polymerization and core-shell polymerization exhibit larger rebinding capacity over the nano particle stabilized emulsion polymerization, the result was a consequence of switching from non-covalent to reversible covalent and overall the molecular imprint effect was not observed.

1 Introduction

Molecular imprinting is an area with a steadily increasing interest [Whitcombe *et al.*, 2014]. The fundamental aspect of a Molecularly Imprinted Polymer (MIP) is to construct ligand selective recognition sites in a polymer network assisted by the presence of a site organizing molecule, termed template, during polymerization [Alexander *et al.*, 2006]. This specific recognition is reminiscent of biological antibody receptors and is therefore often referred to as plastic antibodies or antibody mimics [Hoshino *et al.*, 2008; Vlatakis *et al.*, 1993; Bowen *et al.*, 2013]. An attractive advantage of MIP over biological receptors is their long shelf life and tolerance to harsh treatment, for example: organic solvents, high temperature, acid and bases [Kriz & Mosbach, 1995]. Development of MIPs has been aimed at a wide range of applications including: solid-phase extraction [Guo *et al.*, 2008; Chen & Zhang, 2008; Lasakova & Jandera, 2009], assays [Greene Nathaniel *et al.*, 2004; Ikawa *et al.*, 2006], sensors [Selvolini & Marrazza, 2017; Pietrzyk *et al.*, 2009; Khan *et al.*, 2016], membranes [Silvestri *et al.*, 2006; Wu *et al.*, 2010], catalysis [Busi *et al.*, 2004; Huang *et al.*, 2004], drug delivery [Alvarez-Lorenzo & Concheiro, 2004], and *in vivo* sequestration of toxins [Hoshino *et al.*, 2010]. Typically a complex is formed between the template and a monomer, termed the functional monomer. The steric configuration of the formed complex is then consolidated and set in a polymer matrix by polymerization in the presence of cross linker. Molecular imprinting has been achieved through a number of approaches: a) Reversible covalent. Here the template is covalently bound to one or more polymerizable groups. The polymerization and subsequent template extraction then leaves behind a cavity with functionality capable of re-establishing the covalent bond [Wulff *et al.*, 1985]. b) Semi-covalent. Resembling covalent imprinting the template is first covalently bound by mononer and polymerized, but the functional group left in the cavity after template extraction does not re-establish a covalent bond with the template but interacts non covalently [Whit-

combe *et al.*, 1995]. c) Non-covalent. Here the binding consists of intermolecular interaction such as hydrogen bonding, ion pairing and dipole-dipole [Nomura *et al.*, 1998]. d) Metal ion-mediated. Here a transition metal ion is complexed by polymerizable ligand. The complexed transition metal ion can then coordinate the template [Striegler, 2001]. Protic solvents are often avoided both during imprinting and rebinding due to the competition for hydrogen bonding [Mayes & Mosbach, 1996; Ramström & Ansell, 1998]. The solvent for imprinting is an important consideration, as molecules can have different configurational preferences in varying solvents [Karabulut & Leszczynski, 2013] and the polymer can exhibit different swelling property affecting rebinding sites. Thus, rebinding is often observed to work best in the same solvent as the molecule was initially imprinted in [Vasapollo *et al.*, 2011]. The molecular imprinting of saccharides is of special interest since cheap and robust recognition can aid in blood glucose monitoring for diabetic patients [Yoshimi *et al.*, 2009] and early cancer detection [Wang *et al.*, 2016; Jin *et al.*, 2010]. For *in vivo* use or direct application, a solvent change before rebinding is not applicable, and molecular imprinting in water is thus desirable. Molecular imprinting is traditionally done in bulk polymerization [Peeters *et al.*, 2012; Alenus *et al.*, 2013; Kirk *et al.*, 2009]. Dependant on the application, for example chromatography, further processing of the bulky material into smaller particles is usually needed. While sieving the particles will afford a reasonably narrow polydispersion, a lot of material will go to waste and the obtained particles are usually of non uniform shape giving them poor packing ability with limited to no control over their colloidal behaviour [Kellens *et al.*, 2016]. Hence, a polymerization procedure that affords particles without the need for post processing would be beneficial. In this study Alizarin Red S (ARS) was chosen as template molecule due to its chromophoric nature making it easy to detect and bearing resemblance towards monosaccharides in the form of a 1,2-diol. In this study three different methodologies for the synthesis of molecularly imprinting particles were explored with the goal of selective rebinding of saccharides under aqueous conditions using ARS as a model analyte.

2 Nano Particle Stabilized Emulsion Polymerization

A conversion from bulk to particle while maintaining the properties of the bulk polymerization can be achieved with an emulsion. In this study, a pickering emulsion is utilized; a technique which, in essence, consists of a large number of discrete bulk polymerizations. In bulk polymerization, partitioning coefficients primarily lead to low solubility since there is no secondary phase to migrate to. However, an emulsion consists of two phases and therefore it becomes important to reconcile the partition coefficients of the monomer/template mixture. Because every component of the polymerization needs to be in the same phase, a hydrophilic monomer composition was required. To this end, Acrylamide (AAm) and N-Hydroxymethyl Acrylamide (HMAAm) was chosen as functional monomers with Methylene Bisacrylamide (BIS) as the crosslinker. Ammonium Persulfate (APS) was used as initiator with N,N,N,N-Tetramethyl-Ethylenediamine (TEMED) as catalyst. The molecular structures are shown in Figure 2. ARS has 2 hydrogen bond donor/acceptor sites and 5 acceptor sites. ARS also has an ionic charge, but ionic interaction will not be considered here. AAm has 1 hydrogen bond donor/acceptor site and 1 acceptor site. HMAAm has 2 hydrogen bond donor/acceptor sites and 1 acceptor site. A 1:3 molar ratio of AAm to HMAAm gives 7 donor sites matching the 7 acceptor sites of ARS and a surplus of acceptor sites. To shift the equilibrium towards complexion of template a functional monomer:template ratio of (2:6):1 was chosen. To achieve a bulk like dispersed phase, it is essential to stabilize the emulsion against coalescence during the polymerization. A pickering emulsion describes an emulsion stabilized by particles adsorbed at the oil/water interface. Using particles to stabilize is a matter of a three part interfacial surface tension: oil-water, solid-oil and solid-water. Under partial wetting conditions, the free energy of adsorption for a spherical particle is given by:

$$\Delta_{ads}F = -\pi\ R^2\gamma o - w(1 \pm\ cos(\theta_W)) \quad (1)$$

were R is the particle radius, $\gamma o - w$ the oil-water surface tension and θ_W the particle contact angle in water. The $\pm$ depends on θ_W, $-$ for $\theta_W < 90^o$ and $+$ above [Chevalier & Bolzinger, 2013]. Unlike typical surfactants, particles do not decrease the interfacial surface tension. Stabilization is instead provided mainly in the form of steric repulsion [Vignati *et al.*, 2003].

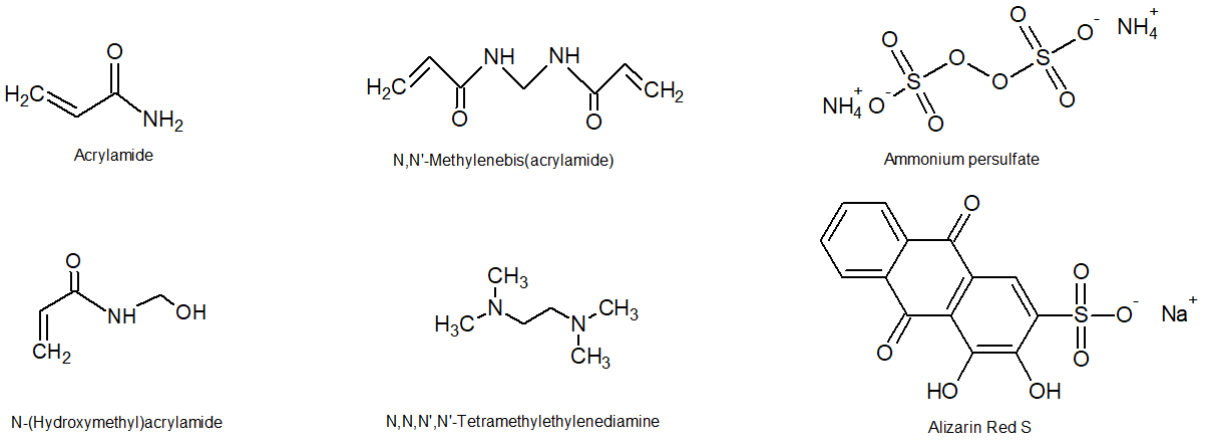

Figure 2: Molecular structure for the reagents used in the pickering emulsion polymerization.

Figure 1: Optical images of silica particles with an added drop of demineralized water. Left side is the unmodified silica were the water drop is adsorbed and wetting the powder. On the right is the DCDMS-modified silica. Here the drop of water does not wet the particles but instead maintains a high contact angle.

Surface modified silica nano particles were chosen for the emulsion. Modification was necessary since silica, by nature, is too hydrophilic to meet the partical wetting requirement. This failure would cause it to remain dispersed in the water phase rather than adsorb at the water/oil interface. A shift in Hydrophilic-Lipophilic Balance (HLB) was achieved through silanization of silica, changing surface hydroxyl groups to dimethylsilyl with Dichlorodimethylsilane (DCDMS). The change is demonstrated in Figure 1. Here, the high contact angle obtained between DCDMS-silica and a water droplet can be seen. The solubility of ARS is relatively low, 1g/L (Sigma Aldrich), but in the presence of Phosphate Buffered Saline (PBS)(7.4pH), 34.2mg (0.1mM) was about the solubility limit. Attempts at the previously mentioned stoichiometry failed to produce solid structures. As the pickering emulsion was disrupted during particle retrieval and washing, the droplets collapsed and disappeared. The low monomer concentrations likely lead to a droplet containing oligomers rather than a crosslinked hydrogel. Increasing the monomer to the amount used by Shen *et al.* [2012] afforded a studier structure, but left the monomer:template ratio at 3500:1. This also had BIS at ≈6.6 % way below the usual 80-90 % crosslinker [Kellens *et al.*, 2016]. The emulsion was formed by vigorously shaking the reaction vessel once both phases had been mixed. As this was done by hand, the shear rate might have been insufficient in creating the large water/oil interface as indicated by the particle size distribution shown in Figure 3. The produced MIP particles had a slight entrapment of template resulting in a faint pinkish colour after template removal.

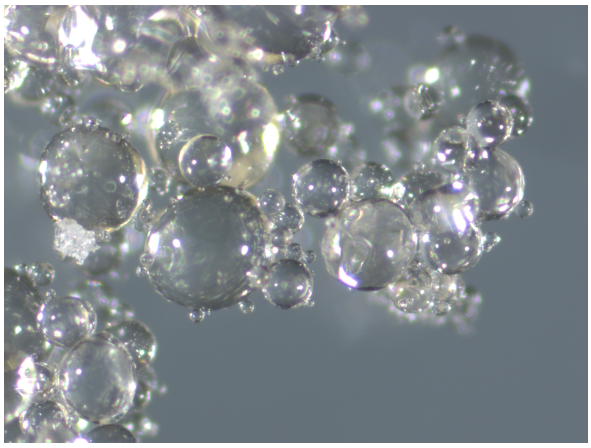

Figure 3: Optical images of particles obtained from pickering emulsion polymerization. The large particles are about 200 μm across and in their dry state.

3 Conventional Emulsion Polymerization

The limited solubility of ARS was an obstacle for the all in one phase molecular imprinting by pickering emulsion polymerization. The second strategy aims to alleviating this problem by means of a conventional emulsion polymerization. The key point of a conventional emulsion polymerization is that the monomer should be soluble in the dispersed phase while the initiator should be soluble in the continuous phase. This separation makes conventional emulsion polymerization a rather unique and complex process. Where before the continuous phase served only as an inactive separator here it becomes an active part of the polymerization process. Only the case with a surfactant concentration above Critical Micelle Concentration (CMC) will be considered in the following as it is the method used. Monomer is distributed between large monomer droplets and small monomer swollen micelles. Initially, water borne free radicals react with the monomer spatially dissolved in the aqueous phase producing a radical oligomer. Upon reaching a critical size, it becomes absorbed into the dispersed phase. The monomer swollen micelles will dominate in this absorption given their mere number and associated surface area compared to the monomer droplets. The micelle absorbing the radical oligomer will thus become a particle nuclei. The continuous growth of these particles is supported by diffusion of monomer from the large monomer droplets. The growing particles increase the oil-water interface area thus requiring more surfactant to maintain stability. This extra surfactant is provided by disbanding unnucleated micelles and from the surface of monomer droplets. The nucleation stage ends when all micelles are gone. The nucleated particles continue to grow until depletion of monomer droplets results in polymerization completion [Chern, 2006]. For the emulsion polymerization, 4-Vinylphenylboronic Acid (VPBA) was the functional monomer, Ethylene Glycol Dimethacrylate (EGDMA) the crosslinker, ARS the template, APS the initiator and Sodium Dodecyl Sulfate (SDS) the surfactant. This approach aims at utilizing the transfer of monomer from droplet deposits to starved reaction loci during the polymerization. During diffusion across the continuous phase, the functional monomer comes into contact with the template. If a complex is formed between the two and the HLB and stability of this new complex is suitable for absorption at the reaction loci and subsequent polymerization, this allows for an imprinting by template transportation as depicted in Figure 5. This would greatly increase the amount of ARS available during polymerization since the continuous phase acts as a large deposit. To achieve this, a boronic acid diol complex is utilized. Boronic acids are known to complex molecules containing diol moieties through the formation of reversible ester bonding [Springsteen & Wang, 2002]. This has been utilized as key element in both sensors and transporters for saccharides [Alexeev *et al.*, 2004; Cambre & Sumerlin, 2011; Draffin *et al.*, 2001].

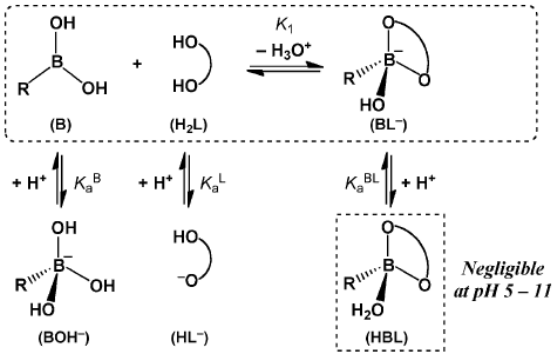

Figure 4: The main reaction between boronic acid and a diol in the 5-11 pH range. The side reactions shown makes the equilibrium pH dependant. [Furikado *et al.*, 2014]

In aqueous solutions at pH 5-11, the reaction between boronic acid and a diol containing ligand can be described by the main reaction occurring (Figure 4). This reaction can be described by Eq. 2

$$K' = \frac{K_1}{[H^+] + K_a^B + K_a^L + (K_a^B K_a^L / [H^+])} \quad (2)$$

Here K' is the conditional formation constant which is pH dependant, K_1 is the equilibrium constant unique to the reaction in question, K_a^B and K_a^L are the acid dissociation constants for boronic acid and the diol respectively. A max K' is reached at pH=$(pK_a^B + pK_a^L)/2$ [Furikado *et al.*, 2014]. Given a pK_a^L of 5.3 for ARS [Furikado *et al.*, 2014] and a pK_a^B of 8.8 for VPBA [Vancoillie & Hoogenboom, 2016], a max K' is reached at pH≈7.

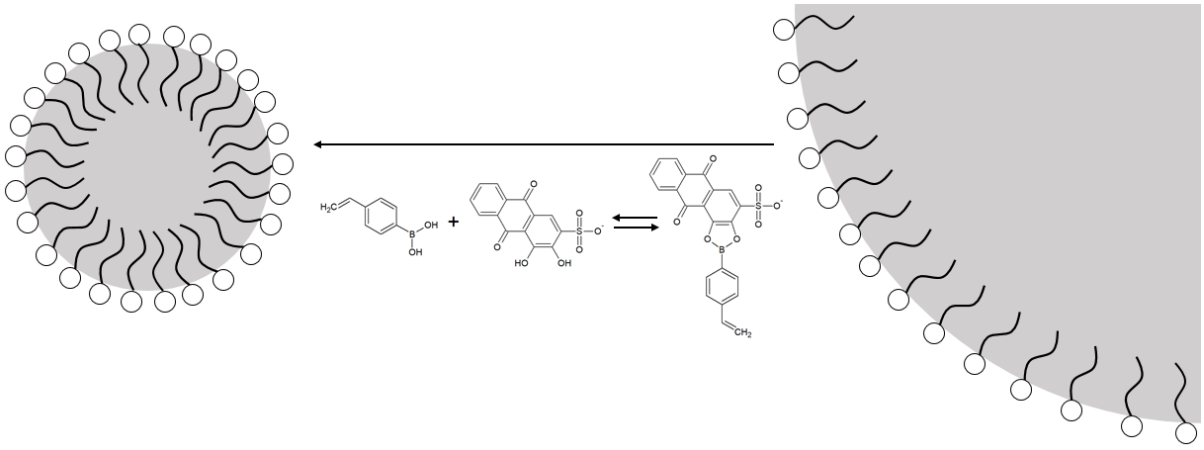

Figure 5: A depiction of the molecular transporting system. Monomer diffusion across the continuous phase, from large droplets (Right) to starved reaction loci (left), results in interaction with, and complexation of, template molecules present in the continuous phase.

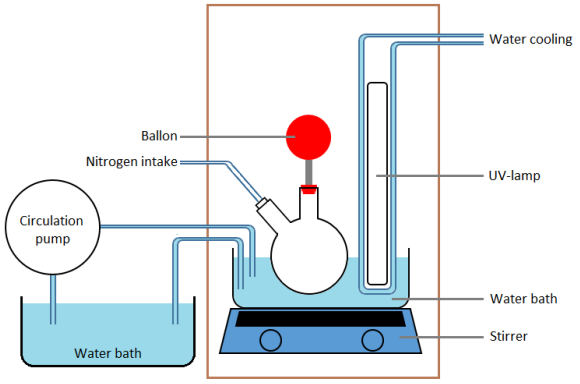

Figure 6: Sketch of the constructed photoreactor. Being build from pre-existing apparatus, it consisted of an enclosure containing an UV-lamp, a magnetic stirrer and a water bath. Outside the enclosure was a larger water bath and a pump to enable temperature control.

This strategy circumvents the concept of a pre-polymerization complex. The non covalent interaction for this system is weak. If ARS is bound by VPBA, it will not have any hydrogen bond donor sites and only acceptors. EGDMA does not posses any hydrogen bond donors, and will be unable to create hydrogen bonds with a ARS:VPBA complex. This puts the majority of imprinting effect on the covalent binding between ARS and VPBA with EGDMA providing preference through steric competitor exclusion. The higher concentration of EGDMA in the dispersed phase would cause it to be the primary monomer for propagation during the initial growth. VPBA is predicted to be about six times more soluble in water than EGDMA [ACD/Labs, 2016]. This difference in partition coefficients would cause a further concentration difference between VPBA and EGDMA in favour of the latter in the particle nucleus. This could give the particles a gradient structure with the concentration of VPBA going from low to high from centre to surface and vice versa for EGDMA. This is favourable since it would concentrate the imprinting sites to the surface allowing for fast access [Cutting & Tabner, 1995]. A simple photoreactor was build in order to separate initiator decomposition rate from temperature. A sketch of the setup is shown in Figure 6. Since the reaction was only illuminated from one side, good stirring was crucial to insure homogeneous conditions. But stirring too vigorously could potentially be counter productive as the incorporation of ARS relies primarily on diffusion for monomer transfer. Increased stirring would lead to increased particle-particle interaction and monomer transfer through collision rather than diffusion. During polymerization the particles, swelled to a point were the emulsion was no longer sustainable. The swollen particle slurry proved to viscous for the magnetic stir bar, leaving it unable to move. This caused a heterogeneous photo initiation for the remaining of the polymerization. Attempts were made at controlling the swelling. The process was also attempted with a more hydrophobic crosslinker, divinylbenzene, leaving out both ARS and VPBA. This however yielded similar results and the polymerization was thermally initiated instead to alleviate some of the heterogeneity. The final particles stem from the central slurry excluding the wall fouling. The obtained particles were estimated at 800nm with a polydispersity index of 0.1 by Dynamic Light Scattering (DLS) in ethanol. The polydispersity index

is deflated by loss of smaller non sedimented particles during centrifugation-redispersion steps. The complexation between boronic acid and ARS shifts the chromophore from red to orange-yellow. This was noticed during polymerization indicating the successful interaction between the monomer and template. As the polymerization progressed and the particles grew and swell the solution changed from orange-yellow to white. After template extraction the particles had an almost unnoticeable orange hue.

4 Core-Shell Polymerization

A different approach to molecular imprinting in particles comes in the form of surface imprinted core-shell particles. Reducing the imprinting area to the outer layer of a particle could potentially aid in mass transfer which is a problem for MIPs [Wulff, 2013; Tan & Tong, 2007]. This involved a two step polymerization with a bit of prep work. First, silanization of silica nano particles to add two functional groups, methacrylate and an Atom-Transfer Radical-Polymerization (ATRP) initiator. Then the VPBA were polymerized, creating a brush structure on the particles by ATRP. Next, ARS were fixated by the chains of VPBA and a shell was polymerized, attaching to the methacrylate groups for the non covalent imprinting, after which the template was removed, finalizing the imprinted core-shell particles. A schematic overview can be seen in Figure 7. ATRP is a Controlled/living Radical Polymerization (CRP) technique and the most popular one when it comes to grafting polymer brushes, partly for its ease of surface initiator fixation [Xu *et al.*, 2014; Matyjaszewski & Spanswick, 2005]. It utilizes a transition metal complex to alternately activate and deactive radicals [Matyjaszewski & Xia, 2001]. This causes only a fraction of the chains to be active at any one time, decreasing the chance of two radicals meeting and thus terminating. If chain transfer is avoided the polymerization allows for living chains of narrow size distribution [Heuts *et al.*, 1999]. Alternatively to direct surface growth, well defined polymer chains could be synthesised by CRP using with clickable initiators for subsequent attachment with surface fixated click groups [Mansfeld *et al.*, 2010]. Ideally the poly(VPBA) brush structure should swollen during polymerization to allow the access of template and monomer. For imprinting in the polymer brush, finishing the shell, non-covalent interaction was used with hydrophilic monomers HMAAm and BIS. A stoichiometric approach was not possible since while the exact amount of ARS bound by the poly(VPBA) brushes could potentially be measured, the polymerization is not bulk and both shell and free oligomers would be present. This technique aims to create a composite shell with rebinding sites distributed along well defined polymer chains locked in different polymer matrix organised by molecular imprinting.

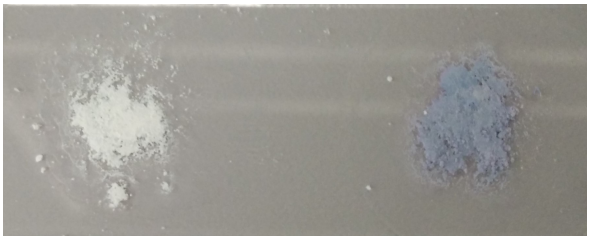

Figure 8: Optical images of silica particles treated with ninhydrin solution. Left side is the unmodified silica which remains white. Right side is the modified silica dyed blue by the ninhydrin due to the presence of primary amines

A simultaneous double silanization of nano silica particles was performed using (3-Aminopropyl)trimethoxysilane and 3-(Trimethoxysilyl)propyl methacrylate in ethanol. The process involved hydrolysis of the methoxy groups into hydroxyl groups followed by condensation between silica surface hydroxyl groups and the newly created hydroxyl groups. (3-Aminopropyl)trimethoxysilane serves as both a reactant and a base catalyst in the reaction. The surface primary amines were then substituted with 2-Bromoisobutyryl Bromide (BIBB) catalysed by triethylamine. ATRP was performed with Cu as transition metal and Tris[2-(dimethylamino)ethyl]amine as ligand, with a ratio of 40:1:1.2 monomer:copper:ligand. The success of the silanization and subsequent initiator fixation was confirmed by treating samples with a ninhydrin solution. Figure 8 shows the treated silica having a blue colour caused by the presence of the primary amine group [Fox & Fiddler, 1984]. When the ATRP initiator surface fixed silica was subjected to the ninhydrin test, a negative result was obtained, with the powder remaining white, indicating the absence of primary amines. The ninhydrin test is very sensitive and detects minor amounts of primary amine. While this is useful for the qualitative determination of the conversion of amines, it does not reveal the actual amount present on the surface. The presence of methacrylate groups on the surface were not confirmed.

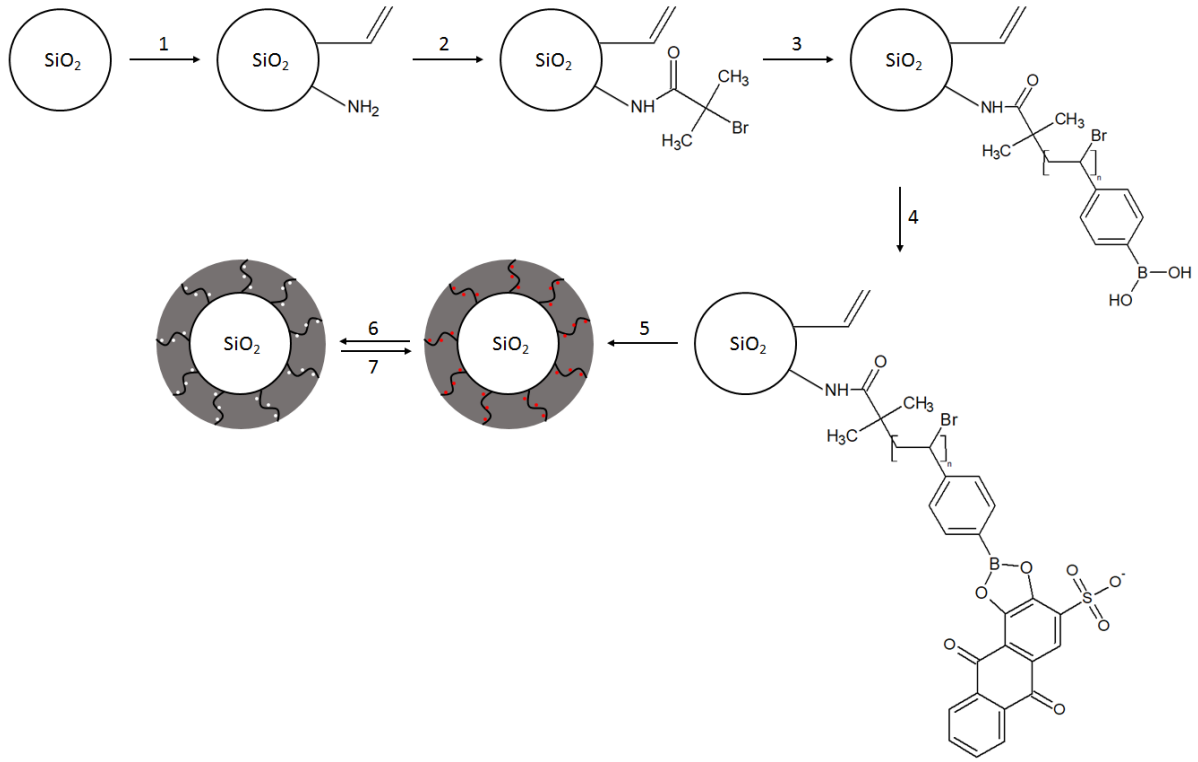

Figure 7: Schematic overview of the core-shell particle synthesis. 1) simultaneous double silanization introducing primary amines and polymerizable vinyl groups to the surface. 2) Converting the primary amines to an ATRP initiator. 3) Creating a surface brush structure by ATRP polymerization of VPBA. 4) Fixation of ARS by covalent bond with the boronic acid moieties of the polymer brushes. 5) Molecular imprinting by interlocking the chains in crosslinked polymer matrix. 6) ARS extraction. 7) ARS rebinding

After ATRP the particle size was estimated to 1.5 μm (in ethanol) by DLS, indicating a large surface brush structure had been achieved. The particles had a very slight greenish hue likely from copper impurities remaining trapped in the polymer. Dispersing They also showed slight hydrophobicity when suspended in water for the shell imprinting. A small amount of SDS and ample stirring provided an apparent homogeneous suspension. After polymerization of the shell the particles did not exhibit hydrophobicity indicating the incorporation of a hydrophilic polymer.

5 Batch Rebind

To asses imprinting effect a batch rebind assay was carried out. The data was converted into points of F (μ M) vs B (μ mol/g) (Figure 9) and fitted with Langmuir, Bi-Langmuir, Tri-Langmuir, Freundlich, LangmuirFreundlich, Redlich-Peterson, Sips and Toth isotherms. This was reduced to the Langmuir (Eq. 3) and the Freundlich isotherm (Eq. 4) since they provided equal fittings with less parameters.

$$B = \frac{B_{max} * F}{K_d + F} \tag{3}$$

Langmuir isotherm is a discrete binding model describing a narrow unimodal distribution of affinity. The two constants B_{max} and K_d can be interpreted as binding site density and dissociation constant.

$$B = a * F^m \tag{4}$$

Freundlich isotherm is a continuous distribution model with parameters a and m. m is a measure of heterogeneity going from one being homogeneous to zero with increasing heterogeneity. a is a combination of binding site density and average affinity. An approximation of the affinity distribution can be with Eq. 5.

$$N(K) = a\frac{sin(\pi\ m)}{\pi}K^{-m} \tag{5}$$

The approximation is only valid within the experimental concentration region, K_{min}-K_{max} defined as $K_{min}=1/F_{max}$ and $K_{max}=1/F_{min}$. The Langmuir and Freundlich isotherm can both be linearized and were fitted on both the linearized and non linearized data points and cross compared. The measure of fitness was evaluated using RMSE, with the error adjusted to per point percentage error, for the non linear plot and R^2 for the linear plots. This showed a consistent better fit obtained from the linear fitting. From the Freundlich fit an affinity distribution can be approximated and the two parameters $N_{K_{min}-K_{max}}$ and $\overline{K}_{K_{min}-K_{max}}$ extracted using Eq. 6 and Eq. 6. All data treatment was done in MATLAB R2015b(8.6).

$$N_{K_{min}-K_{max}} = a(1-m^2)(K_{min}^{-m} - K_{max}^{-m}) \tag{6}$$

$$\overline{K}_{K_{min}-K_{max}} = \frac{m}{m-1}\frac{K_{min}^{1-m} - K_{max}^{1-m}}{K_{min}^{-m} - K_{max}^{-m}} \tag{7}$$

Table 1: The table contains the fitting parameters obtained from linear fitting.

Particle	Langmuir	
PMIP	R^2:	0.950
	RMSE:	17.703
	B_{max}:	1.448
	K_d:	34.113
PNIP	R^2:	0.989
	RMSE:	10.940
	B_{max}:	2.063
	K_d:	68.780
	Freundlich	
EMIP	R^2:	0.976
	RMSE:	8.624
	a:	0.766
	m:	0.670
	$N_{K_{min}-K_{max}}$:	7.540
	$\overline{K}_{K_{min}-K_{max}}$:	0.042
ENIP	R^2:	0.961
	RMSE:	10.427
	a:	1.009
	m:	0.634
	$N_{K_{min}-K_{max}}$:	8.997
	$\overline{K}_{K_{min}-K_{max}}$:	0.044
CMIP	R^2:	0.969
	RMSE:	6.639
	a:	3.415
	m:	0.414
	$N_{K_{min}-K_{max}}$:	13.625
	$\overline{K}_{K_{min}-K_{max}}$:	0.064
CNIP	R^2:	0.962
	RMSE:	7.999
	a:	2.405
	m:	0.479
	$N_{K_{min}-K_{max}}$:	12.547
	$\overline{K}_{K_{min}-K_{max}}$:	0.055

6 Results and Discussion

The difficulty of finding the ideal template:functional monomer ratio highlights one of the main obstacle of non covalent molecular imprinting. Often the optimal polymer formulation is

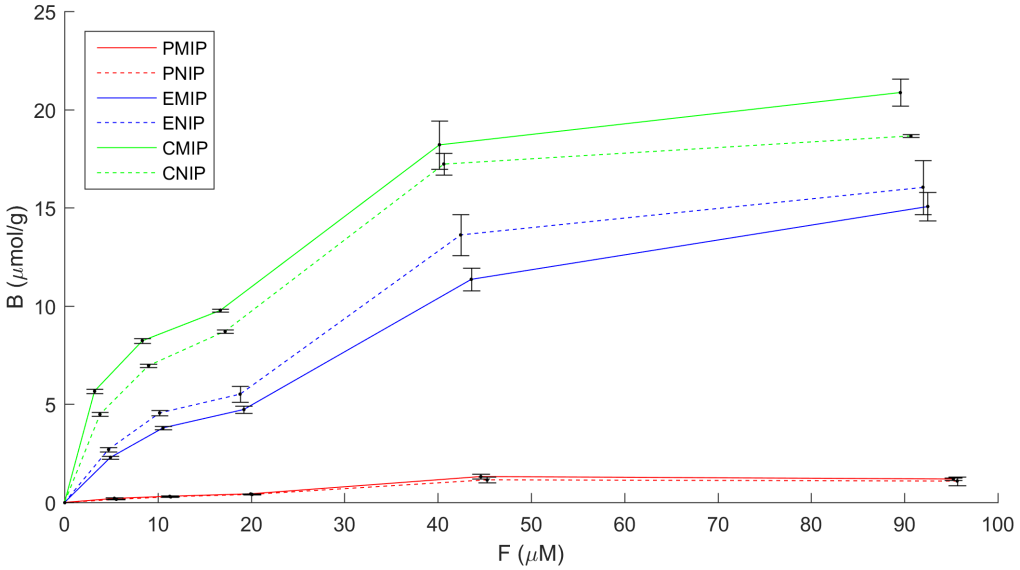

Figure 9: F (μM) vs Bound (μmol/g) with error bars for the particles: Pickering (PMIP), Emulsion (EMIP) Core-Shell (CMIP) (-) and their non imprinted counter parts (PNIP, ENIP, CNIP) (- -). The lines between points are drawn arbitrarily for visual aid.

achieved empirically through numerous attempts adjusting the template:functional monomer ratio [Kim & Spivak, 2003]. While a great knowledge of intermolecular interaction is not necessarily a requirement, the work can be tedious and expensive, depending on the reagents and synthesis. To help alleviate the work load, research has been done in the field of computer-aided design [Liang *et al.*, 2016]. These are, however, often based on a pre-polymerization complex. While such a complex can be demonstrated to exist [Kirk *et al.*, 2009], it is debatable if it prevails through the polymerization and has merit on the final binding site configuration [Kim & Spivak, 2003; Yan & Ho Row, 2006]. Usually the crosslinker constitutes 80-90% of the polymer [Kellens *et al.*, 2016]. BIS used in both the pickering and core-shell particles also posses 2 hydrogen bond donor/acceptor sites and 2 acceptor sites, it should therefore be capable of template interaction and might be a valid point for optimization [Sibrian-Vazquez & Spivak, 2003]. The low solubility of ARS makes it a poor candidate for the pickering emulsion presented in this study. While a 1:3500 ratio of template:functional monomer shifts the equilibrium towards a complex it also causes a large number of non complexed monomer. The reverse action of increasing the template to large ratio might seem better since any excess template will not be a part of the final polymer. However, this might also cause complications. Propose a template and monomer combination exhibiting both a 1:1 and a stronger 1:2 template:monomer complex. A large excess in template would shift the equilibrium towards the weaker 1:1 complex. The pickering emulsion offers new possibilities. The ease of silica surface modification allows for fixation of a template, making pure surface imprinting achievable [Shen & Ye, 2011]. The large neighbouring of silica bound to the template would allow for the simultaneous imprinting of a range of molecules possessing the imprinted moiety. The emulsion particles were not fully realised due to manufacturing difficulties. It does, however, hold a lot of potential as a one step particle producing molecular imprinting technique that allows for the incorporation of an approximate 1:1 binding site:functional monomer ratio for diol containing templates. While the optimal pH for complexion between ARS and VPBA at pH of 7 would allow reasonable function *in vivo* at pH 7.4 [Kellum, 2000], monosaccharides have much higher pK_a values of up to around 12. To counter balance the shift in optimal pH to the alkaline region, lower pK_a value boronic acid derivatives have been synthesised [Lauer & Wulff, 1983; Roberts *et al.*, 2007]. Saturation of surface bound poly(VPBA) in the core-shell particles by template before shell imprinting could be further enforced by anhydrous distillation [Yoshimi *et al.*, 2009]. However, self condensation of boronic acid forming boroxines can also occur [Nishiyabu *et al.*, 2011]. While the living ends of the poly(VPBA) chains afforded by

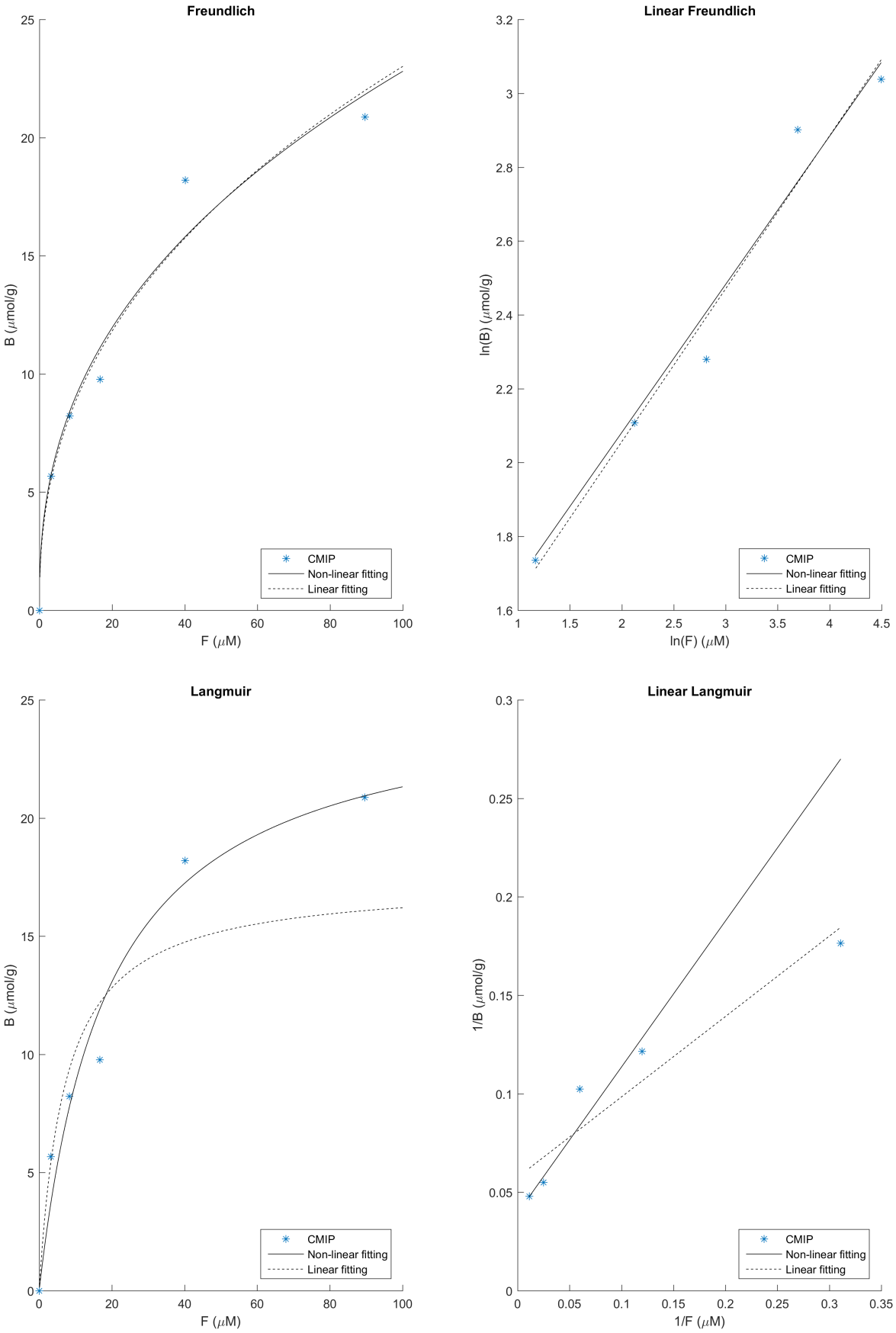

Figure 10: The Langmuir model and Freundlich model are both cross fittet on the same data points of CMIP. There is good consistency between the linear and non-linear Freundlich while Langmuir shows deviation.

ATRP are left unused this study, their could be utilized for controlling colloidal ability of the core-shell particles. The nature of molecular imprinting results in a heterogeneous continuous distribution of binding sites [Mattiasson & Ye, 2015]. Reminiscent of the Maxwell-Boltzmann distribution, it is asymmetric with a maxima of weak binding sites and a decaying curve going towards a few strong binding sites. Imprinting should shift the distribution towards stronger binding sites. Under the assumption that not more, but instead stronger, binding sites are created the skewed affinity distribution flattens. The Langmuir isotherm models for essentially one specific affinity constant and capacity. In terms of a heterogeneous polymer this means fitting to the maxima of the affinity distribution. Since the incorporation of stronger binding sites flattens the affinity distribution, this maxima becomes less pronounced and the Langmuir model less useful. The Freundlich isotherm models for a continuous distribution and therefore fits this affinity distribution better, provided the collected data does not approach saturation. Fitting both linear and non linearly for subsequent cross comparing showed the inappropriateness of the Langmuir model for the emulsion and core-shell particles as the fit yielded poor results when compared to its counterpart on top of vastly varying parameters (Figure 10). The Langmuir fits were fairly consistent for the pickering particles. The last two data points of rebinding for the pickering particles also indicates them approaching saturation. This gave the Langmuir model an edge over Freundlich for the fitting since Freundlich does not fit saturation. While the PMIP has a lower binding site density, compared to the PNIP, its dissociation constant is about half that of the PNIP indicating a stronger binding. The Freundlich model gave a reasonable fit (R^2>0.95) and consistent parameters for the emulsion and core-shell particles. Having the particles described by two different models is very reasonable as the Pickering is purely non covalent while the emulsion and core-shell particles also have covalent binding properties. A Langmuir fit for the pickering particles also suggest a narrow distribution of weak bonding. The larger binding site density ($N_{K_{min}-K_{max}}$), higher heterogeneity (m) and greater weighted average affinity ($\overline{K}_{K_{min}-K_{max}}$) of the CMIP over the CNIP indicates a modest imprinting effect [Rampey *et al.*, 2004]. However, the reverse observation for the EMIP and ENIP sows doubt for the indicated imprinting effect of the CMIP. Boronic acid shows specific high affinity reversible binding of diols and incorporating it into a polymer network would naturally lead to a higher binding affinity. Since this affinity is applied towards effectively all diol containing molecules in general, the cavity creation of molecular imprinting should aim to exclude competitors. The imprinting effect might have been better elucidated in competitive rebinding with a suitable analogue for the template.

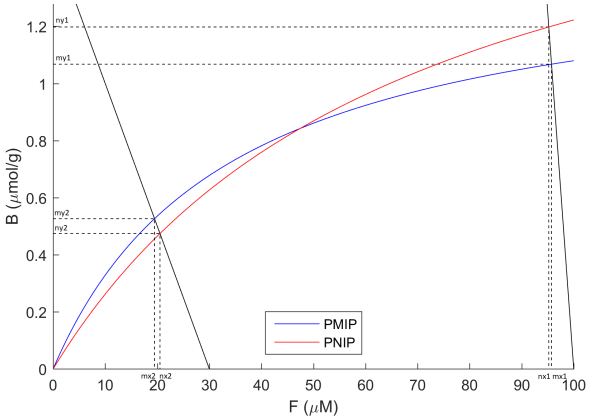

Figure 11: F (μM) vs Bound (μmol/g) for PMIP and PNIP.

The different strategies of molecular imprinting, as well as the abundance of methods employed to make sense of the data, makes quantifying molecular imprinting a difficult task. The imprinting factors calculated are generally a poor indicator for molecular imprinting since they differ vastly with experimental settings [Castell *et al.*, 2011; Lasakova & Jandera, 2009]. The imprinting factor is a single point experimental value. Figure 11 shows the fitted curves for PMIP and PNIP along with the cross points used to calculate the imprinting factor for two single points. The right most point is at 0.1 mM template concentration while the left is at 0.0125 mM, both with 5 mL volume and 20 mg particle. The imprinting factors calculated are 0.89 for the right and 1.24 for the left. This indicates an optimal working condition for the MIP but also highlights the problem of only reporting a single imprinting factor as the result. As with all other fields, molecular imprinting also has less than reliable claims of success and critique of data collection and treatment has been raised [Verheyen *et al.*, 2011].

7 Conclusion

Three different particles, pickering, emulsion and core-shell, were synthesised. The core-shell particles showed the highest capacity for rebinding. Pickering emulsion polymerization was not found fit for the imprinting of a low soluble template such as ARS. This method, however, hold potential for mono- and disaccharides with a much higher solubility. Molecular imprinting by template transportation was attempted in an emulsion polymerization and while the adsorption capacity was higher than for the pickering particles, the molecular imprinting effect was not observed, and the process needs further optimization for stable uniform particle formation. The core-shell particles indicated a doubtful imprinting effect. While they exhibit the greatest rebinding capacity this was somewhat offset by their complicated synthesis. A truer measure of their imprinting effect needs to be evaluated.

8 Procedure

8.1 Materials

N-Hydroxymethyl Acrylamide, N,N,N,N-Tetramethyl-Ethylenediamine, Alizarin Red S, Ethylene Glycol Dimethacrylate, Sodium Dodecyl Sulfate, Copper(I) Bromide, 2-Bromoisobutyryl Bromide, Acrylamide/Bis-Acrylamide, 40% Solution, (3-Aminopropyl)trimethoxysilane, Tetrahydrofuran, Hydrofluoric Acid and Ninhydrin were bought from Sigma Aldrich. *n*-Hexane, Ethanol, Acetonitrile and Toluene were bought from VWR International. Dichlorodimethylsilane and 3-(Trimethoxysilyl)propyl Methacrylate were bought from Fluka. Sodium Chloride, Potassium Chloride, Disodium Phosphate and Monopotassium phosphate were bought from J.T. Baker. 4-Vinylphenylboronic Acid and Tris[2-(dimethylamino)ethyl]amine were bought from TCI chemicals. Ammonium Persulfate was bought from Bie & Berntsen and Triethylamine from Alfa Aesar. All chemicals were used without further purification.

8.2 Pickering

4 g of silica particles were dried in an oven at 150 ℃ for 1 h. Once cooled, to room temperature, they were added to 100 mL *n*-hexane containing 8 mL DCDMS under nitrogen. After stirring overnight, the particles were retrieved by centrifugation and washed with *n*-hexane and ethanol before being dried in an oven at 150 ℃. Two phases were made separately: For the oil phase 300 mg of DCDMS-silica particles where added to 15 mL toluene with 15 mL *n*-hexane in a 50 mL centrifuge tube and sonified for 30 min. For the water phase, a saturated solution of ARS in 1xPBS was made. To 7.45 mL 1xPBS ARS sat. was added 0.645 mL AAm, 2 mL HMAAm and 150 mg BIS. Both phases were kept in an icebath for 10 min before mixing and the solution was vigorously shaken by hand to form the emulsion. After adding 10 mg APS and 8 μ L TEMED the solution was shaken again for 10 sec and left over night. The particles were retrieved by centrifugation and washed with a mix of water and acetonitrile three times. Silica was removed by treatment with dilute hydrofluoric acid. The particles were then washed with slightly acidic water until no ARS was detected in the supernatant by UV-vis and the particles were dried on filter paper. The same procedure was followed for the Non Imprinted Polymer (NIP) omitting the ARS.

8.3 Emulsion

Two phases were prepared separately: A polar phase consisting of 30 mL 1xPBS solution at 0.1 mM ARS to which 100 mg SDS and 75 mg APS were added. For the non-polar phase, 50 mg VPBA was added to 5 mL EGDMA. The two phases were mixed in a round bottom flask in an ice bath. After purging with nitrogen for 10 min under magnetic stirring (400 RPM), the temperature was raised to 80 ℃ for 4 hours. The resulting particles were retrieved and washed by cycles of centrifugation-redispersion in acidic water and ethanol. This was repeated until no ARS was detected in the supernatant by UV-vis. The particles were dried in an oven at 105 ℃ . The NIP followed the same procedure omitting the ARS.

8.4 Core-Shell

2 g of silica nanospheres (250 nm) were suspended in 40 mL ethanol containing 200 μL of (3-Aminopropyl)trimethoxysilane and 3-(Trimethoxysilyl)propyl methacrylate in a polypropylene vessel with circular shaking overnight. The particles were retrieved cycles of centrifugation-redispersion and washed with ethanol and dried under vacuum. 1 g of silanizated silica particles was mixed in 1.6 mL triethylamine and 24 mL tetrahydrofuran and cooled in an ice−water bath. 1.2 mL BIBB was added drop-

wise to the solution. The temperature was then raised to 25 ℃ and reaction was stirred overnight. The particles were retrieved by centrifugation and washed with ethanol, and dried under vacuum. 3 g of initiator fixated particles were suspended in 150 mL 2-propanol in a 250 mL 3 neck round bottom flask to which 3.5 g VPBA was added. The flask was equipped with a condenser topped with a balloon, a nitrogen inlet and a septum. The mixture was stirred under a continuous nitrogen flow for 1 h. Meanwhile 0.085 g of CuBr and 190 μL Tris[2-(dimethylamino)ethyl]amine were mixed in 50 mL 2-propanol in a 100 mL 1 neck round bottom flask in an anaerobic glove box and sealed with a septum. The formed complex was then added to the main solution by syringe and given 10 min of nitrogen flow before being sealed off. The temperature was raised to 90 ℃ and left to stir for 48 h. The particles were retrieved by centrifugation and washed with ethanol, and dried under vacuum. 1 g of polymer brush silica particles was suspended in 210 mL 1xPBS at 0.1 mM ARS. To this 0.1525 g SDS 0.5 BIS and 3.92 HMAAm was added. The solution was stirred under nitrogen while heated to 70 ℃ . 50 mL of APS solution (1 mg/mL) was added to start the reaction and it was kept at 70 ℃ under nitrogen over night. The particles were retrieved by centrifugation and washed with acidic water and ethanol until no ARS was detected in the supernatant and dried under vacuum.

8.5 Batch Rebind

For batch rebind studies, a concentration series was made with ARS in 1xPBS (0.1 mM 0.05 mM 0.025 mM 0.0125 mM 0.00625 mM 0 mM). For the emulsion and core-shell particles 500 mg were dispersed by a sonifier in PBS adding up to a total volume of 30 mL. 150 μL particle solution were added to 5 mL of each concentration step for the rebind row while 150 μL 1xPBS were added to a separate concentration series for comparison, giving 2.5 mg. The pickering particles, being to large for stable dispersion, were instead weighted using 20 mg for each concentration step. A separate a concentration series were made without the added 150 μL 1xPBS for the pickering particles. Three parallel rows were made for each particle type. The solutions were left to incubate at room temperature over night with light shaking. The solutions were then centrifugated, filtered (0.2 μm RC) and an UV absorption spectre were recorded for each using 3 mL solution in a macrocuvette on a UV-vis spectrophotometer (Varian Cary 50 Scan UV Visible Spectrophotometer). The value of the absorption peak occurring between 400 and 600 nm was used for comparison. A single data point was removed from the triplet set at 0.00625 mM for the CNIP, the whole spectrum had massive adsorption deviating heavily from the rest of the set and giving a large negative adsorption.

9 Abbreviations

EGDMA Ethylene Glycol Dimethacrylate

AAm Acrylamide

HMAAm N-Hydroxymethyl Acrylamide

BIS Methylene Bisacrylamide

DCDMS Dichlorodimethylsilane

HLB Hydrophilic-Lipophilic Balance

TEMED N,N,N,N-Tetramethyl-Ethylenediamine

MIP Molecularly Imprinted Polymer

NIP Non Imprinted Polymer

ARS Alizarin Red S

APS Ammonium Persulfate

ATRP Atom-Transfer Radical-Polymerization

VPBA 4-Vinylphenylboronic Acid

BIBB 2-Bromoisobutyryl Bromide

SDS Sodium Dodecyl Sulfate

CMC Critical Micelle Concentration

CRP Controlled/living Radical Polymerization

PBS Phosphate Buffered Saline

DLS Dynamic Light Scattering

PMIP Pickering Molecular Imprinted Polymer

PNIP Pickering Non Imprinted Polymer

EMIP Emulsion Molecular Imprinted Polymer

ENIP Emulsion Non Imprinted Polymer

CMIP Core Shell Molecular Imprinted Polymer

CNIP Core Shell Non Imprinted Polymer

RMSE Root Mean Square Error

References

ACD/Labs (2016): Percepta Platform - PhysChem Module.

Alenus, J., Ethirajan, A., Horemans, F., Weustenraed, A., Csipai, P., Gruber, J., Peeters, M., Cleij, T. J., & Wagner, P. (2013): Molecularly imprinted polymers as synthetic receptors for the QCM-D-based detection of l-nicotine in diluted saliva and urine samples. *Analytical and Bioanalytical Chemistry*, **405** 20: 6479–6487. ISSN 16182642.

Alexander, C., Andersson, H. S., Andersson, L. I., Ansell, R. J., Kirsch, N., Nicholls, I. A., O'Mahony, J., & Whitcombe, M. J. (2006): Molecular imprinting science and technology: A survey of the literature for the years up to and including 2003. *Journal of Molecular Recognition*, **19** 2: 106–180. ISSN 09523499.

Alexeev, V. L., Das, S., Finegold, D. N., & Asher, S. A. (2004): Photonic crystal glucose-sensing material for noninvasive monitoring of glucose in tear fluid. *Clinical Chemistry*, **50** 12: 2353–2360. ISSN 00099147.

Alvarez-Lorenzo, C. & Concheiro, A. (2004): Molecularly imprinted polymers for drug delivery. *Journal of Chromatography B: Analytical Technologies in the Biomedical and Life Sciences*, **804** 1: 231–245. ISSN 15700232.

Bowen, J. L., Manesiotis, P., & Allender, C. J. (2013): Twenty years since 'antibody mimics' by molecular imprinting were first proposed: A critical perspective. *Molecular Imprinting*, **1**: 35–40. ISSN 2084-8803.

Busi, E., Basosi, R., Ponticelli, F., & Olivucci, M. (2004): An innovative approach to the design of plastic antibodies: Molecular imprinting via a nonpolar transition state analogue. *Journal of Molecular Catalysis A: Chemical*, **217** 1-2: 31–36. ISSN 13811169.

Cambre, J. N. & Sumerlin, B. S. (2011): Biomedical applications of boronic acid polymers. *Polymer*, **52** 21: 4631–4643. ISSN 00323861.

Castell, O. K., Barrow, D. A., Kamarudin, A. R., & Allender, C. J. (2011): Current practices for describing the performance of molecularly imprinted polymers can be misleading and may be hampering the development of the field. *Journal of Molecular Recognition*, **24** 6: 1115–1122. ISSN 09523499.

Chen, S. & Zhang, Z. (2008): Molecularly imprinted solid-phase extraction combined with electrochemical oxidation fluorimetry for the determination of methotrexate in human serum and urine. *Spectrochimica Acta - Part A: Molecular and Biomolecular Spectroscopy*, **70** 1: 36–41. ISSN 13861425.

Chern, C. S. (2006): Emulsion polymerization mechanisms and kinetics. *Progress in Polymer Science (Oxford)*, **31** 5: 443–486. ISSN 00796700.

Chevalier, Y. & Bolzinger, M. A. (2013): Emulsions stabilized with solid nanoparticles: Pickering emulsions. *Colloids and Surfaces A: Physicochemical and Engineering Aspects*, **439**: 23–34. ISSN 09277757.

Cutting, G. R. & Tabner, B. J. (1995): Reaction temperature profiles and radical concentration measurements on batch emulsion copolymerization of methyl methacrylate and butyl acrylate. *European Journal of Pharmaceutics and Biopharmaceutics*, **31** 12: 1215–1219.

Draffin, S. P., Duggan, P. J., & Duggan, S. A. M. (2001): Highly fructose selective transport promoted by boronic acids based on a pentaerythritol core. *Organic Letters*, **3** 6: 917–920. ISSN 15237060.

Fox, J. A. Y. B. & Fiddler, R. N. (1984): Ruhemann ' s Purple from Ninhydrin ,. *Bioorganic Chemistry*, **12**: 235–241.

Furikado, Y., Nagahata, T., Okamoto, T., Sugaya, T., Iwatsuki, S., Inamo, M., Takagi, H. D., Odani, A., & Ishihara, K. (2014): Universal Reaction Mechanism of Boronic Acids with Diols in Aqueous Solution: Kinetics and the Basic Concept of a Conditional Formation Constant. *Chemistry - A European Journal*, **20** 41: 13194–13202. ISSN 15213765.

Greene Nathaniel, T., Morgan Stephen, L., & Shimizu Ken, D. (2004): Molecularly imprinted polymer sensor arrays. *Chemical communications (Cambridge, England)*, **10**: 1172–1173. ISSN 1359-7345.

Guo, Z. F., Guo, T. T., & Guo, M. (2008): Preparation of molecularly imprinted adsorptive resin for trapping of ligustrazine from the traditional Chinese herb Ligusticum chuanxiong Hort. *Analytica Chimica Acta*, **612** 2: 136–143. ISSN 00032670.

Heuts, J. P. A., Mallesch, R., & Davis, T. P. (1999): Atom transfer radical polymerization in the presence of a thiol: more evidence supporting radical intermediates. *Macromolecular Chemistry and Physics*, **200** 6: 1380–1385.

Hoshino, Y., Kodama, T., Okahata, Y., & Shea, K. J. (2008): Peptide Imprinted Polymer Nanoparticles : A Plastic Antibody Peptide Imprinted Polymer Nanoparticles : A Plastic Antibody. **130** October: 15242–15243.

Hoshino, Y., Koide, H., Urakami, T., Kanazawa, H., Kodama, T., Oku, N., & Shea, K. J. (2010): Recognition, neutralization, and clearance of target peptides in the bloodstream of living mice by molecularly imprinted polymer nanoparticles: A plastic an-

tibody. *Journal of the American Chemical Society*, **132** 19: 6644–6645. ISSN 00027863.

Huang, J. T., Zheng, S. H., & Zhang, J. Q. (2004): Molecularly imprinting of polymeric nucleophilic catalysts containing 4-alkylaminopyridine functions. *Polymer*, **45** 12: 4349–4354. ISSN 00323861.

Ikawa, T., Hoshino, F., Matsuyama, T., Takahashi, H., & Watanabe, O. (2006): Molecular-Shape Imprinting and Immobilization of Biomolecules on a Polymer Containing Azo Dye Molecular-Shape Imprinting and Immobilization of Biomolecules on a Polymer Containing Azo Dye. *Society*, **22**: 2747–2753.

Jin, S., Cheng, Y., Reid, S., Li, M., & Wang, B. (2010): CarbohydrateRecognition by Boronolectins, Small-Molecules, andLectins. *Medicinal Research Reviews*, **30** 2: 171–257.

Karabulut, S. & Leszczynski, J. (2013): Anomeric and rotameric preferences of glucopyranose in vacuo, water and organic solvents. *Journal of Molecular Modeling*, **19** 9: 3637–3645. ISSN 16102940.

Kellens, E., Bové, H., Conradi, M., D'Olieslaeger, L., Wagner, P., Landfester, K., Junkers, T., & Ethirajan, A. (2016): Improved Molecular Imprinting Based on Colloidal Particles Made from Miniemulsion: A Case Study on Testosterone and Its Structural Analogues. *Macromolecules*, **49** 7: 2559–2567. ISSN 15205835.

Kellum, J. A. (2000): Determinants of blood pH in health and disease. *Crit Care*, **4** 1: 6–14. ISSN 1364-8535.

Khan, M. A. R., T.C. Moreira, F., Riu, J., & F. Sales, M. G. (2016): Plastic antibody for the electrochemical detection of bacterial surface proteins. *Sensors and Actuators, B: Chemical*, **233**: 697–704. ISSN 09254005.

Kim, H. & Spivak, D. A. (2003): New insight into modeling non-covalently imprinted polymers. *Journal of the American Chemical Society*, **125** 37: 11269–11275. ISSN 00027863.

Kirk, C., Jensen, M., Kjaer, C. N., Smedskjaer, M. M., Larsen, K. L., Wimmer, R., & Yu, D. (2009): Aqueous batch rebinding and selectivity studies on sucrose imprinted polymers. *Biosensors and Bioelectronics*, **25** 3: 623–628. ISSN 09565663.

Kriz, D. & Mosbach, K. (1995): Competitive amperometric morphine sensor based on an agarose immobilised molecularly imprinted polymer. *Analytica Chimica Acta*, **300** 1-3: 71–75. ISSN 00032670.

Lasakova, M. & Jandera, P. (2009): Molecularly imprinted polymers and their application in solid phase extraction. *Journal of Separation Science*, **32** 5-6: 799–812. ISSN 16159306.

Lauer, M. & Wulff, G. (1983): Arylboronic acids with intramolecular B-N interaction: convenient synthesis through ortho-lithiation of substituted benzylamines. *Journal of Organometallic Chemistry*, **256** 1: 1–9. ISSN 0022328X.

Liang, D., Wang, Y., Li, S., Li, Y., Zhang, M., Li, Y., Tian, W., Liu, J., Tang, S., Li, B., & Jin, R. (2016): Study on Dicyandiamide-Imprinted Polymers with Computer-Aided Design. *International Journal of Molecular Sciences*, **17** 11: 1750. ISSN 1422-0067.

Mansfeld, U., Pietsch, C., Hoogenboom, R., Becer, C. R., & Schubert, U. S. (2010): Clickable initiators, monomers and polymers in controlled radical polymerizations – a prospective combination in polymer science. *Polymer Chemistry*, **1** 10: 1560. ISSN 1759-9954.

Mattiasson, B. & Ye, L. (2015): *Molecularly imprinted polymers in Biotechnology*, volume 150. ISBN 4411334364.

Matyjaszewski, K. & Spanswick, J. (2005): Controlled/living radical polymerization. *Materials Today*, **8** 3: 26–33. ISSN 13697021.

Matyjaszewski, K. & Xia, J. (2001): Atom transfer radical polymerization. *Chemical reviews*, **101** 9: 2921–2990. ISSN 00092665.

Mayes, A. G. & Mosbach, K. (1996): Molecularly Imprinted Polymer Beads: Suspension Polymerization Using a Liquid Perfluorocarbon as the Dispersing Phase. *Analytical Chemistry*, **68** 21: 3769–3774. ISSN 0003-2700.

Nishiyabu, R., Kubo, Y., James, T. D., & Fossey, J. S. (2011): Boronic acid building blocks: tools for self assembly. *Chem Commun*, **47** 4: 1124–1150. ISSN 1359-7345.

Nomura, Y., Muguruma, H., Yano, K., Kugimiya, A., McNiven, S., Ikebukuro, K., & Karube, I. (1998): Selective Recognition of 2,4-Dichlorophenoxyacetic Acid Using a Molecularly Imprinted Polymer. *Analytical Letters*, **31** 6: 973–980. ISSN 0003-2719.

Peeters, M., Troost, F. J., Van Grinsven, B., Horemans, F., Alenus, J., Murib, M. S., Keszthelyi, D., Ethirajan, A., Thoelen, R., Cleij, T. J., & Wagner, P. (2012): MIP-based biomimetic sensor for the electronic detection of serotonin in human blood plasma. *Sensors and Actuators, B: Chemical*, **171-172**: 602–610. ISSN 09254005.

Pietrzyk, A., Suriyanarayanan, S., Kutner, W., Chitta, R., & D'Souza, F. (2009): Selective histamine piezoelectric chemosensor using a recognition film of the

molecularly imprinted polymer of bis(bithiophene) derivatives. *Analytical Chemistry*, **81** 7: 2633–2643. ISSN 00032700.

Rampey, A. M., Umpleby, R. J., Rushton, G. T., Iseman, J. C., Shah, R. N., & Shimizu, K. D. (2004): Characterization of the Imprint Effect and the Influence of Imprinting Conditions on Affinity, Capacity, and Heterogeneity in Molecularly Imprinted Polymers Using the Freundlich Isotherm-Affinity Distribution Analysis. *Analytical Chemistry*, **76** 4: 1123–1133. ISSN 00032700.

Ramström, O. & Ansell, R. J. (1998): Molecular imprinting technology: Challenges and prospects for the future. *Chirality*, **10** 3: 195–209. ISSN 08990042.

Roberts, M. C., Hanson, M. C., Massey, A. P., Karren, E. A., & Kiser, P. F. (2007): Dynamically restructuring hydrogel networks formed with reversible covalent crosslinks. *Advanced Materials*, **19** 18: 2503–2507. ISSN 09359648.

Selvolini, G. & Marrazza, G. (2017): MIP-based sensors: Promising new tools for cancer biomarker determination. *Sensors (Switzerland)*, **17** 4. ISSN 14248220.

Shen, X. & Ye, L. (2011): Interfacial molecular imprinting in nanoparticle-stabilized emulsions. *Macromolecules*, **44** 14: 5631–5637. ISSN 00249297.

Shen, X., Zhou, T., & Ye, L. (2012): Molecular imprinting of protein in Pickering emulsion. *Chemical Communications*, **48** 66: 8198. ISSN 1359-7345.

Sibrian-Vazquez, M. & Spivak, D. A. (2003): Enhanced enantioselectivity of molecularly imprinted polymers formulated with novel cross-linking monomers. *Macromolecules*, **36** 14: 5105–5113. ISSN 00249297.

Silvestri, D., Barbani, N., Cristallini, C., Giusti, P., & Ciardelli, G. (2006): Molecularly imprinted membranes for an improved recognition of biomolecules in aqueous medium. *Journal of Membrane Science*, **282** 1-2: 284–295. ISSN 03767388.

Springsteen, G. & Wang, B. (2002): A detailed examination of boronic acid-diol complexation. *Tetrahedron*, **58** 26: 5291–5300. ISSN 00404020.

Striegler, S. (2001): Selective discrimination of closely related monosaccharides at physiological pH by a polymeric receptor. *Tetrahedron*, **57** 12: 2349–2354. ISSN 00404020.

Tan, C. J. & Tong, Y. W. (2007): Molecularly imprinted beads by surface imprinting. *Analytical and Bioanalytical Chemistry*, **389** 2: 369–376. ISSN 16182642.

Vancoillie, G. & Hoogenboom, R. (2016): Synthesis and polymerization of boronic acid containing monomers. *Polym Chem*, **7** 35: 5484–5495. ISSN 1759-9954.

Vasapollo, G., Sole, R. D., Mergola, L., Lazzoi, M. R., Scardino, A., Scorrano, S., & Mele, G. (2011): Molecularly imprinted polymers: Present and future prospective. *International Journal of Molecular Sciences*, **12** 9: 5908–5945. ISSN 14220067.

Verheyen, E., Schillemans, J. P., Van Wijk, M., Demeniex, M. A., Hennink, W. E., & Van Nostrum, C. F. (2011): Challenges for the effective molecular imprinting of proteins. *Biomaterials*, **32** 11: 3008–3020. ISSN 01429612.

Vignati, E., Piazza, R., & Lockhart, T. P. (2003): Pickering emulsions: Interfacial tension, colloidal layer morphology, and trapped-particle motion. *Langmuir*, **19** 17: 6650–6656. ISSN 07437463.

Vlatakis, G., Andersson, L. I., Müller, R., & Mosbach, K. (1993): Drug assay using antibody mimics made by molecular imprinting. *Nature*, **361** 6413: 645–647. ISSN 0028-0836.

Wang, S., Yin, D., Wang, W., Shen, X., Zhu, J.-J., Chen, H.-Y., & Liu, Z. (2016): Targeting and Imaging of Cancer Cells via Monosaccharide-Imprinted Fluorescent Nanoparticles. *Scientific Reports*, **6** March: 22757. ISSN 2045-2322.

Whitcombe, M. J., Kirsch, N., & Nicholls, I. A. (2014): *Molecular imprinting science and technology: A survey of the literature for the years 2004-2011*, volume 27. Wiley. ISBN 1021502000885.

Whitcombe, M. J., Rodriguez, M. E., Villar, P., & Vulfson, E. N. (1995): A New Method for the Introduction of Recognition Site Functionality into Polymers Prepared by Molecular Imprinting: Synthesis and Characterization of Polymeric Receptors for Cholesterol. *Journal of the American Chemical Society*, **117** 27: 7105–7111. ISSN 0002-7863.

Wu, S., Tan, W., & Xu, H. (2010): Protein molecularly imprinted polyacrylamide membrane: for hemoglobin sensing. *The Analyst*, **135** 10: 2523. ISSN 0003-2654.

Wulff, G. (2013): Fourty years of molecular imprinting in synthetic polymers: Origin, features and perspectives. *Microchimica Acta*, **180** 15-16: 1359–1370. ISSN 00263672.

Wulff, G., Oberkobusch, D., & Minárik, M. (1985): Enzyme-analogue built polymers, 18 chiral cavities in polymer layers coated on wide-pore silica. *Reactive Polymers, Ion Exchangers, Sorbents*, **3** 4: 261–275. ISSN 01676989.

Xu, Z., Deng, P., Tang, S., & Li, J. (2014): Fluorescent boronic acid terminated polymer grafted silica particles synthesized via click chemistry for affinity separation of saccharides. *Materials Science and Engineering C*, **40** I: 228–234. ISSN 09284931.

Yan, H. & Ho Row, K. (2006): Characteristic and Synthetic Approach of Molecularly Imprinted Polymer. *Int J Mol Sci*, **7**: 155–178. ISSN 1422-0067.

Yoshimi, Y., Narimatsu, A., Nakayama, K., Sekine, S., Hattori, K., & Sakai, K. (2009): Development of an enzyme-free glucose sensor using the gate effect of a molecularly imprinted polymer. *Journal of Artificial Organs*, **12** 4: 264–270. ISSN 14347229.

Appendix

Emulsion polymerization

Nano Emulsion

Different ratios of Tween 80, chloroform and water were mixed to determine the nano emulsion region. This was done by mixing Tween 80 and water first and then dropwise add the chloroform under vigorous stirring. While this provided stable emulsions they were not nano emulsion. Sonification was used to provide shear instead as the shear rate of stirring was thought insufficient. A low powered rod initially yielded indifferent results. A higher power let not to nano emulsion but close as an almost transparent solution was obtained. Switching the chloroform to EGDMA caused slight coagulation from partial polymerization within a minute even with ice cooling due to the high powered sonification. Prolonged sonification using short burst intervals lowered the degree of polymerization but did not yield a nano emulsion. It was decided to abstract from nano particles to plain particles.

Emulsion

EDGMA, VPBA and Alizarin was mixed together and added to a water phase containing Tween 80 and APS. The pH was measured and adjusted to neutral. The solution was bubbled with nitrogen and polymerization was initiated by UV for 24 h. After polymerization the resulting translucent solution showed no large polymer particles. Upon extended centrifugation a small solid phase collected. After repeatable steps of centrifugation and re dispersion. The resulting assumed particle suspension was dried in an oven 105 ℃. This resulted in the formation of hard flakes that could not be re dispersed. Thinking that the heat of the oven might have been to much the polymerization was re attempted. When adjusting the pH from slightly acidic to neutral by addition NaOH, black precipitate was formed on contact, failing to reproduce the original observations the procedure was set on hold. The focus was switched to a water soluble template ARS and a template transfer imprinting process was proposed. These early attempts and subsequent failures at imprinting in emulsion polymerization for this study can be summarized as "greed". Working at the very limit with supersaturated solutions in order to force as much template as possible into the polymer led to failed polymerizations time after time. Realizing that pH measurements of an emulsion is questionable and the instead opting to use a buffer for controlling the pH and reducing the amount of ARS making sure everything was dissolved immediately led to a much better polymerization. Where before it was a struggle to retrieve anything from the post polymerization mixture it was now filled to the brim with polymer. This however caused a complete blockage for the magnetic stirring. The polymerization was attempted thermally instead. Varying Amounts of Tween 80, SDS and combinations hereof were attempted to stabilize the emulsion polymerization. However, the result did not chance significantly. It was decided to stick with one surfactant as to not induce competitive micelle nucleation. As the resultant mixture was not a solid but just very heavily packed with particles it was decided to increase the ratio of monomer:water by lowering the amount of monomer. This yielded similar results. reaching low monomer to water ratio it became clear that the particles were swollen since the extra space between particles allowed for increased swelling. The particles were not stable in their swollen state and was gradually reduced to smaller fragments with more vigorous stirring. The particles obtained from the heavily packed slurry at 5:30 volume ratio of monomer:water was washed and dried in an oven at 105 ℃. These particles remained as a fine powder and did not form flakes as observed previously. As a side note it might have been optimal not to dry any of the polymers as not to disrupt binding site structure by deswelling. However, it was the most convenient way of obtaining particle weight for batch rebind experiment.

Pickering

Surface modification was done by drying silica particles in an oven before suspending them in a mixture of hexane and dichlorodimethylsilane in a glove box. After over night stirring the solution was milky as the particles were now more hydrophobic. After washing the particles were dried in an oven. The particles had not been properly washed as small holes had formed in the aluminium tray used for the drying

indicating that HCl had been formed from dichlorodimethylsilane reacting with water. The washing had been done with a mix of hexane and ethanol. The particles were re washed and subsequent runs made sure to was 3 times with hexane before switching phase to ethanol for drying. Hexane, toluene and surface modified silica particles were mixed and sonificated for 30 min, meanwhile ARS, AAm, HMAAm, BIS and APS were mixed in PBS. The two solutions were mixed, shaken and the formed emulsion was transferred to a 2-neck round bottom flask with a magnetic stir bar. After bubbling with nitrogen for 10 min, the polymerization was initiated by UV for 24 h. The polymerization resulted in a large lump of hydrogel. No trace of spherical particles in the lump were detected under a microscope. The stirring was omitted and TEMED was used for initiation. Nitrogen bubbling was also omitted. This resulted in stable hydrogel particles. Attempts at stoichiometric monomer:template ratios did not result in stable hydrogels, the concentration likely to low to produce might more than oligomers. Rhodamine B was also attempted as a temple molecule. A range of increased crosslinker content were done from 100 mg to 600 mg. More crosslinker lead to slightly smaller particles with a more rigid and less gel like structure. No change was observed above 150 mg crosslinker, except for Rhodamine B, and the higher amounts also lead to increased undissolved crosslinker. Increasing the amount of crosslinker lead to increasingly smaller particles for the emulsion containing Rhodamine B. Cutting down the time of sonification for the hydrophobic phase seemed to increase the amount of non-spherical particles having egg shape or protrusions.

Polymer Network

The entrapped ARS observed gave the idea for a simple examination of the polymer network. A bulk polymer was created with the same composition as the pickering particles. After extraction of template by soxhlet, the polymer was submerged in an acidic solution. This caused a gradual outside-in colour chance with a fairly defined front. The result was back and forth reversible. This indicated that while template remained trapped in the polymer network it was not completely encapsulated as it was solvent accessible. With a complete colour change occurring within a couple of hours it was it was decided that a 24 hour incubation time would be sufficient for template rebinding.

Soxhlet

Soxhlet extraction was done with methanol on the pickering particles over night but no ARS was detected in the extraction liquid. It was determined that the previous extraction was sufficient.

Core-Shell

Surface modification of silica

A row of single silanizations of silica surface by (3-Aminopropyl)trimethoxysilane at different concentrations was made. After overnight reaction the silica particles were grounded by centrifugation and the supernatant was invested for unreacted (3-Aminopropyl)trimethoxysilane by addition of a ninhydrin. The goal was to estimate the density of hydroxyl groups on the surface of silica allowing for the silanization. Even at very low amounts left over (3-Aminopropyl)trimethoxysilane was detected. It was concluded that the high sensitivity of ninhydrin coupled with the double functionality of (3-Aminopropyl)trimethoxysilane as both reagent and catalyst - making the concentration of reagent and catalyst decrease during the reaction - caused the method to be inappropriate. Attenuated total reflectance fourier-transform infrared spectroscopy were done on silica, aminopropyl-silica and ATRP initiator fixed silica. The study was inconclusive. A method for accessing the presence of bromide on the initiator fixated particles were developed, by hydrolysis and precipitation with silver nitrate solution. a slight turbidity indicated its presence but the amount of bromide/g particle was low and as such the method required too much a mass to be of worth. Attempts at double silanization initially let to polymerization of the of the reagents resulting in large solid lump in place of the fine silica powder. The concentrations of (3-Aminopropyl)trimethoxysilane and 3-(Trimethoxysilyl)propyl methacrylate were lowered through several attempts until the no polymerization was observed. The resulting particles still gave a positive result with the ninhydrin solution. When subjected to 2-bromoisobutyryl bromide the solution

got the look of milk gone sour, but after a while it cleared up and looked as it had done with the single silanization. This is the only clue that methacrylate groups were present on the silica surface.

ATRP

The reaction was intended to run for 48 hours but one day in it was clear that the reactor was not properly sealed. The leak was too small to detect with soap since it took more than 8 hours for the balloon to deflate. Components were switched and the system retested multiple times until the leak was eliminated and the reactor finally overcame more than 48 hours. The particles retrieved from the first reaction were very green indicating a large contamination by the copper. For consistency of the later intended MIP and NIP a large batch of ATRP was created. The resulting particles had a had a slight brownish colour when wet and almost white when dry.

Batch Rebind

Measuring the light absorbance of Rhodamine B, resulted in very (absurdly) high and distorted absorption peaks until a very low concentration was reached making rebinding hard to asses. Micro-cuvettes holding 1 mL volume were initially used. Highly varying data points were observed and it was later determined that the sample holder was not tight enough for consistent measurement as merely flicking the cuvette inbetween measurement produced vastly different results. This rendered earlier data collection invalid.

Data Threatment

Rebinding with of ARS at a constant concentration and varying amounts of emulsion polymer caused a shift in pH confirming the presence of boronic acid but also shifting the UV-vis spectre. A row of ARS at varying pH were collected. The spectres were decomposed into Gaussian line profiles in an attempt to clarify the different excitation states of ARS (Figure 12). This was done with in MATLAB with a custom written function utilizing MATLABs implementation of an unconstrained multivariate function for minimum search.

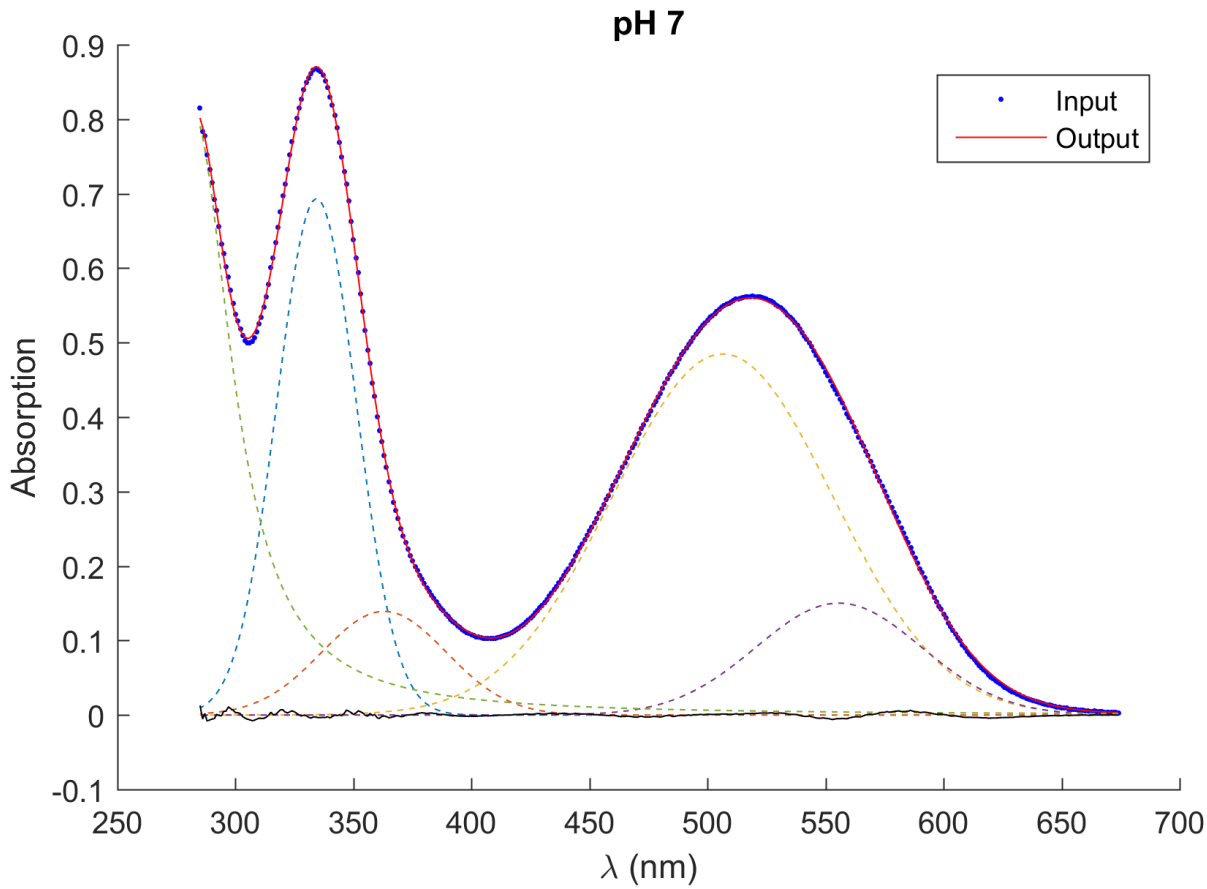

Figure 12: Spectre decomposition for Alizarin Red S. Fitted with Gaussian line profiles for the peaks and a Lorentzian for the background slope.